

## Original Research Article

# UAV Target Detection under Complex Sky Background

Yang Yin<sup>1</sup>, Yang Liu<sup>1</sup>, Shuai Chen<sup>2\*</sup>, Quanshun Yang<sup>1</sup>

<sup>1</sup> School of Electrical Engineering, Naval University of Engineering, Wuhan 430032, Hubei Province, China

<sup>2</sup> No. 710 R&D Institute, CSSC, Yichang 443003, Hubei Province, China

## ABSTRACT

At present, unmanned aerial vehicles (UAVs) are widely used in various fields, and the management of UAVs is very important to solve the problems in the field of low-altitude safety. Due to the low flying height, small radar cross section, and inconspicuous characteristic signals of UAVs, the detection of UAVs based on video frames taken by fixed cameras cannot meet the existing requirements in terms of tracking speed and recognition accuracy. This paper proposes a multi-sensor fusion model. Firstly, the UAV target signal is improved by spatial filtering and improved Sobel operator edge detection algorithm, and then Gaussian filter is used to denoise, and finally the UAV small target is extracted based on the maximum inter-class variance method threshold segmentation algorithm. Experimental results show that this method can effectively enhance the UAV target signal in a complex environment, and the threshold segmentation method also has good adaptability, and can effectively screen UAVs under a complex sky background.

**Keywords:** Small Target Detection; Multi-sensor Fusion Model; Improved Sobel Operator; Threshold Segmentation

## ARTICLE INFO

Received: Jun 30, 2022

Accepted: Oct 11, 2022

Available online: Oct 22, 2022

## \*CORRESPONDING AUTHOR

Shuai Chen

522395342@qq.com

## CITATION

Yin Y, Liu Y, Chen S, Yang Q. UAV Target Detection under Complex Sky Background. Journal of Autonomous Intelligence 2022; 5(2): 1–12. doi: 10.32629/jai.v5i2.514

## COPYRIGHT

Copyright © 2022 by author(s).

Journal of Autonomous Intelligence is published by Frontier Scientific Publishing. This work is licensed under the Creative Commons Attribution-NonCommercial 4.0 International License (CC BY-NC 4.0).  
<https://creativecommons.org/licenses/by-nc/4.0/>

## 1. Introduction

In recent years, a variety of birds, kites, especially unmanned aerial vehicles (UAVs), and other moving objects in the air frequently appear, making the environment at a low altitude increasingly complex. This brings security risks and threats to power transmission lines, communication facilities and special areas that are exposed outdoors for a long time. Therefore, the detection and tracking of UAVs under the sky background is an urgent problem to be solved to ensure safety at low altitude<sup>[1]</sup>. When a UAV is flying in the sky, its flying altitude is low, the radar cross section (RCS) is small, and the flying speed is slow. Driven by a battery-powered motor, UAVs' infrared characteristics are not obvious. The maximum effective signal range can be up to 5–7 km, which makes the sound characteristics and wireless communication signals not obvious during long-distance flight<sup>[2,3]</sup>. The characteristic of the use of UAVs and the characteristics of their flying targets have brought great challenges to the prevention and control of illegal activities of UAVs.

At present, the existing detection methods for small moving objects in a low altitude range are mainly based on target detection of video frames shot by a fixed camera. Although this method is easy to install and easy to operate, it still has two limitations. 1) The fixed camera has a limited field of view, and there is often a tracking loss problem for moving objects, that is, moving objects move out of the monitoring range. 2) As the target object is small, the real-time target detection

cannot meet the requirements, and the accuracy of the traditional segmentation algorithm is poor and prone to misidentification. Therefore, in order to improve the monitoring range of the detection system and the accuracy of target segmentation, this paper aims to carry out real-time detection and monitoring of UAVs under the sky background based on multi-sensor information fusion combined with machine vision and other methods. This method has the advantages of flexible operation, high efficiency and low environmental requirements, which is beneficial to solve the practical application problems in the field of low altitude safety.

The remainder of this paper is organized as follows. In the second chapter, a multisensory information fusion model is proposed to obtain the multi-dimensional characteristic information of a small moving target in the sky background, especially the video images containing the target. In the third chapter, an improved gradient detection and threshold segmentation algorithm are proposed based on the video images to obtain the possible UAV targets in the images. In the fourth chapter, the model and method proposed in this paper are verified by building an experimental platform.

## 2. Information fusion to find targets

### 2.1 Multi-sensor information fusion scheme

Through the fusion of multi-source detection information, the limitation of a single sensor can be made up. The information acquired by multiple sensors has redundancy, which can improve the accuracy of the description of target characteristics, and prevent the influence of partial information missing or error on the decision-making of the whole system. The information obtained by multiple sensors is complimentary at the same time, which enriches the information of different characteristics of the target, effectively improves the recognition ability of the system, and extends the coverage of time and space.

When a single sensor detects the UAV target, it often has some shortcomings such as low accuracy, poor real-time performance and weak anti-interference ability. For example, when detecting

UAV targets, radar can get the distance, direction, speed and other information of targets in the low altitude range, but it cannot distinguish birds, balloons and other targets. Photoelectric equipment can get the appearance information of the target to distinguish UAVs, but it cannot meet the requirements of large-scale and long-distance monitoring at the same time, making it difficult to capture the picture of the suspicious target. Radio frequency (RF) and audio detection equipment are easily interfered with by the surrounding environment, and the detection distance is short. Through analysis and experimental tests, this paper adopts the fusion method which is mainly composed of photoelectric equipment and radar information and assisted by RF signals<sup>[4-6]</sup>. In the case of ensuring the accuracy of characteristic information acquisition, the detection coverage and real-time performance are improved. After the fusion, the information basically meets the necessary conditions for the determination of UAV target invasion.

Based on the multi-source information fusion theory, this paper proposes a multiple sensor information fusion method for linkage control of target detection radar and photoelectric equipment, namely the radar equipment continuously scans low-altitude targets within a range, and captures the basic characteristics of suspicious targets of illegal invasion in real time, including distance, height, direction and speed. When the radar observes the appearance of a small target in the sky, it first transmits its distance, direction and other information to the control center; if there is a suspected UAV target, the control center will be included in the list to be detected according to the distance of the suspicious target; otherwise, the radar will continue to scan and monitor.

According to the radar, the control center provides information such as the distance and direction of the target in the list to be detected, rotates the Pan-Tilt of the photoelectric device, adjusts the direction angle and pitch angle, and the photoelectric device performs zoom and focus at the same time to obtain an image containing suspicious targets. Radio frequency (RF) detection equipment begins to detect the suspicious target and the RF signal in the surrounding area, and judges whether there is a drone

intrusion based on the image information and communication signals<sup>[7]</sup>.

When multiple sensors work at the same time, registration is required first, including time registration and space registration. For time registration, generally speaking, the working cycle of radar is relatively long and the response time of other equipment is relatively short, so the embodiment of the present invention follows the radar time as the standard. For spatial registration, the spatial coordinate systems of different sensing devices are different, and information fusion can only be carried out after the coordinate systems are registered. Based on the Euler Angle, the coordinates of different devices are converted to improve the accuracy of target information matching (as shown in **Figure 1**).

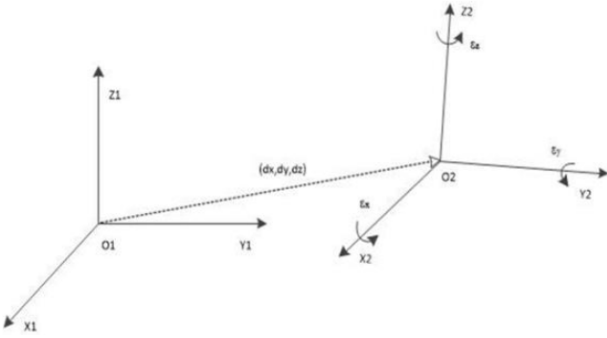


**Figure 1.** Coordinate system transformation.

Take radar equipment and photoelectric Pan-Tilt equipment as an example. If the three-dimensional space coordinate systems of the two equipment are respectively  $O_1X_1Y_1Z_1$  and  $O_2X_2Y_2Z_2$ , according to the order of rotation around  $O_1Z_1$ ,  $O_1Y_1$  and  $O_1X_1$ , the Euler angles corresponding to  $X$ ,  $Y$  and  $Z$  axes are respectively  $\varepsilon_x$ ,  $\varepsilon_y$ ,  $\varepsilon_z$ , and their corresponding rotation matrices  $M_x$ ,  $M_y$ ,  $M_z$  are respectively:

$$M_x = \begin{bmatrix} 1 & 0 & 0 \\ 0 & \cos \varepsilon_x & \sin \varepsilon_x \\ 0 & -\sin \varepsilon_x & \cos \varepsilon_x \end{bmatrix} \quad (1)$$

$$M_y = \begin{bmatrix} \cos \varepsilon_y & 0 & -\sin \varepsilon_y \\ 0 & 1 & 0 \\ \sin \varepsilon_y & 0 & \cos \varepsilon_y \end{bmatrix} \quad (2)$$

$$M_z = \begin{bmatrix} \cos \varepsilon_z & \sin \varepsilon_z & 0 \\ -\sin \varepsilon_z & \cos \varepsilon_z & 0 \\ 0 & 0 & 1 \end{bmatrix} \quad (3)$$

Then the coordinate transformation equation from the radar coordinate system to the photoelectric equipment coordinate system is:

$$\begin{bmatrix} x_A \\ y_A \\ z_A \end{bmatrix} = M_x M_y M_z \begin{bmatrix} x_B \\ y_B \\ z_B \end{bmatrix} = M \begin{bmatrix} x_B \\ y_B \\ z_B \end{bmatrix} \quad (4)$$

Generally speaking, after the equipment is aligned in the same direction during installation, there is little difference between the rotation angle of radar and photoelectric equipment. When the value of  $\varepsilon_x$ ,  $\varepsilon_y$ ,  $\varepsilon_z$  is relatively small, the coordinate transformation formula can be simplified as:

$$\begin{bmatrix} x_A \\ y_A \\ z_A \end{bmatrix} = M \begin{bmatrix} x_B \\ y_B \\ z_B \end{bmatrix} = \begin{bmatrix} 1 & \varepsilon_z & -\varepsilon_y \\ -\varepsilon_z & 1 & \varepsilon_x \\ \varepsilon_y & -\varepsilon_x & 1 \end{bmatrix} \begin{bmatrix} x_B \\ y_B \\ z_B \end{bmatrix} \quad (5)$$

After registering information such as the coordinates of different detection sources, based on the basic fusion theory of information fusion such as the basic decision level, characteristic level, and data level, this paper uses a hybrid structure model to detect small UAV targets under the sky background. The model is shown in **Figure 2**.

The multi sensors first detect the invasion of small targets of UAVs, then obtain the position, speed and other information through the radar sensor, and then obtain the picture and communication signal containing a suspicious target through photoelectric equipment and radio frequency detector. Finally, the system decides whether there is an invasion of UAVs.

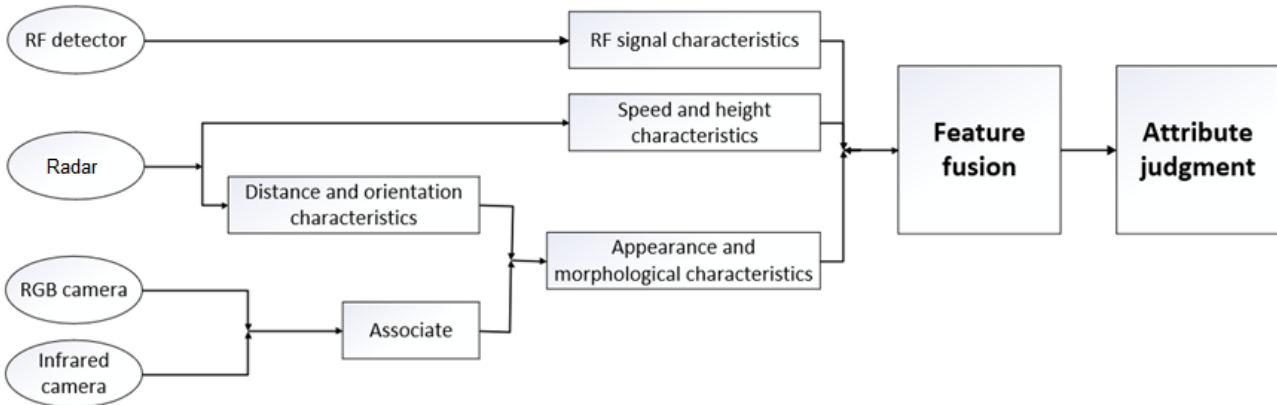


**Figure 2.** UAV detection fusion structure model.

The decision-making process of anti-UAV low-altitude defense is similar to the multi-characteristic attribute decision-making problem. It is a process to evaluate the threat degree of the target by using various characteristics of the target and different characteristics. When the system starts to work, the UAV target that is suspected of illegal intrusion is detected as  $x_i \in \{x_1, x_2, \dots, x_n\}$ , and a decision is made whether to interfere with the target. The judgment basis is that  $m$  characteristic attributes  $Q_i \in \{Q_1, Q_2, \dots, Q_m\}$  of each target are obtained through information fusion. Generally, in the judgment process of UAVs,  $Q_1, Q_2, \dots, Q_m$  respectively represent the distance, height, speed, appearance and other characteristics of the suspicious target, and each attribute is independent of the other. By establishing the relationship between the attribute and the decision, the best result is selected to decide whether to implement countermeasures by interfering with the equipment. At present, the vast majority of UAVs show similar characteristics in the operation process, with a flight height between 100–500 m, and a movement speed between 3–15 m/s. According to the height characteristic  $Q_1$  and velocity characteristic  $Q_2$  of the target obtained by the radar, filter out the target  $x_i \in \{x_1, x_2, \dots, x_t\}$  whose value is in the range of  $100 < q_1 < 500$ ,  $3 < q_2 < 15$ , and the target is used as the list of targets to be detected. Then, the threat degree of the target is judged according to the distance  $Q_3$  and orientation characteristics  $Q_4$  of the target, and the appearance information of the target is obtained by adjusting the orientation angle, pitch angle and zoom ratio of the

photoelectric equipment according to the threat degree.

## 2.2 Analysis of UAV target characteristics

This paper analyzes the video and image information of a large number of small UAV targets under the sky background by shooting and observes that the basic characteristics of small targets' shape, size and average gray level are different from the main interference such as noise and cloud edges. This lays the foundation for the detection and extraction of small targets.

### 2.2.1 Morphological scale characteristics

In the case of remote detection by photoelectric equipment, the size of UAVs is generally less than  $50 \times 50$  (in  $1920 \times 1080$  resolution image), and the proportion of target diagonal in the whole image is generally less than 3%. In addition, beyond the horizontal range of 500–800 m, the morphological characteristics of UAVs such as propeller and bracket are not obvious, so characteristic detection and characteristic matching do not have wide applicability.

### 2.2.2 Area signal-to-noise ratio

The regional grayscale signal-to-noise ratio is used to reflect the relationship between the signal intensity of the target area and the surrounding area, reflecting the signal intensity of the target in the specified area in the grayscale image. Generally speaking, the larger area signal-to-noise ratio (SNR)

is, the more obvious the target in the region is and the less difficult it is to be segmented. The SNR gain is the ratio of the SNR of the output and input images, which is used to reflect the effectiveness of the algorithm. The higher the SNR gain, the better the effect of the algorithm on background suppression and target enhancement.

$$S/N = \frac{|G_t - G_b|}{std_b} \quad (6)$$

$$(S/N)_G = \frac{(S/N)_{out}}{(S/N)_{in}} \quad (7)$$

Note:

$S/N$ : local signal-to-noise ratio;

$(S/N)_G$ : signal-to-noise ratio gain;

$G_t$ : the gray average value of the pixels in the target area;

$G_b$ : the gray average value of the pixel points in the background area;

$std$ : the standard deviation of gray value within the region.

### 2.2.3 Directional gradient characteristic

The directional gradient characteristic in the image is a local characteristic. For high-resolution images, the direct extraction of characteristics requires a large amount of calculation, with poor effect and non-obvious characteristics. Combine with the image pyramid to calculate the directional gradient characteristics of small UAV targets and cloud background interference:

$$F(x, y) = \sqrt{Gra_x^2 + Gra_y^2} \quad (8)$$

$$\alpha(x, y) = |\arctan\left(\frac{Gra_y}{Gra_x}\right)| \in [0, \frac{\pi}{2}) \quad (9)$$

Note:

$F(x, y)$ : the amplitude of the gradient;

$\alpha(x, y)$ : the direction of the gradient;

$Gra_x, Gra_y$ : the gradient values in  $x$  and  $y$  directions calculated by the operator.

In the same image, there is a certain difference between the gradient characteristics of the small target and the background. The magnitude of the gradient is larger, and the gray value changes more than the surrounding environment; the value of the gradient direction is generally left, right, and horizontal, simultaneously with the change in the vertical gradient. The gradient characteristics of background interference are often gradual, with relatively small amplitude, and it usually shows that the value change in one direction is greater than the other. The difference is shown in **Figure 3**.



**Figure 3.** Differences in gradient characteristics between the UAV and background.

## 3. Visual segmentation of moving small targets

### 3.1 Improved Sobel operator gradient detection

The gray value of a UAV target changes obviously in the image. The extraction of gradient characteristics can effectively enhance the target signal. The traditional Sobel discrete difference operator is often used for image gradient extraction, which uses the convolution block to calculate the gray difference of 8 pixels around the pixel point to obtain the edge characteristics of the target. In this paper, an improved operator is proposed based on the traditional algorithm, which increases the sensitivity of the operator to the horizontal and longitudinal edges respectively, expands the detection range of pixels, and reduces the influence of UAV morphological pores on the target signal.

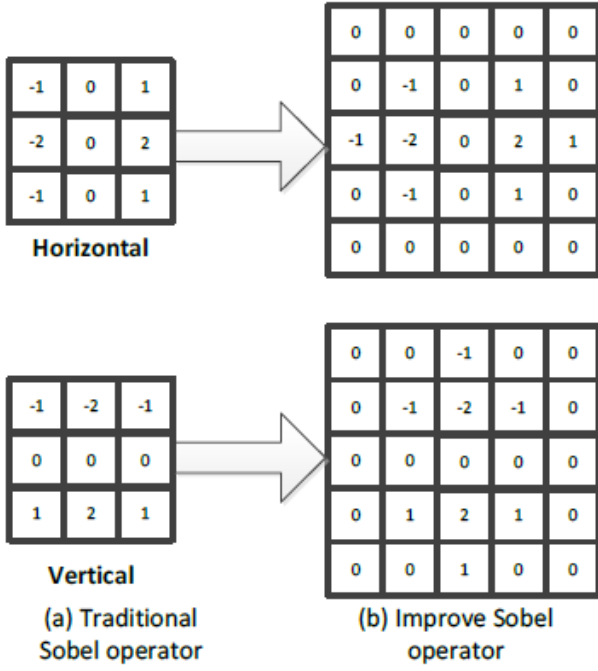


**Figure 4.** Schematic diagram of the improved Sobel operator.

The pixel value in the  $5 \times 5$  range around a certain pixel is:

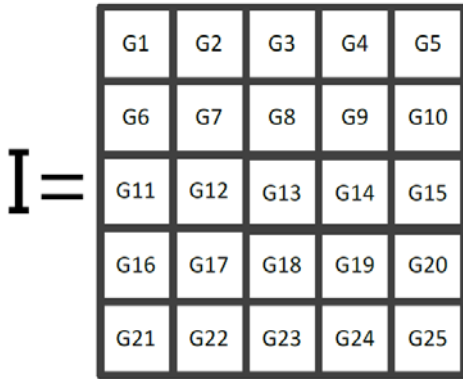


**Figure 5.**  $5 \times 5$  pixel grid number.

Lateral gradient detection formula is:

$$\begin{aligned}
 Gra_x &= \begin{pmatrix} 0 & 0 & 0 & 0 & 0 \\ 0 & -1 & 0 & 1 & 0 \\ -1 & -2 & 0 & 2 & 1 \\ 0 & -1 & 0 & 1 & 0 \\ 0 & 0 & 0 & 0 & 0 \end{pmatrix} \begin{pmatrix} G_1 & G_2 & G_3 & G_4 & G_5 \\ G_6 & G_7 & G_8 & G_9 & G_{10} \\ G_{11} & G_{12} & G_{13} & G_{14} & G_{15} \\ G_{16} & G_{17} & G_{18} & G_{19} & G_{20} \\ G_{21} & G_{22} & G_{23} & G_{24} & G_{25} \end{pmatrix} \\
 &= (2G_{14} + G_9 + G_{15} + G_{19}) - (2G_{12} + G_7 + G_{11} + G_{17})
 \end{aligned} \tag{10}$$

Longitudinal gradient detection formula:

$$\begin{aligned}
 Gra_y &= (2G_{18} + G_{17} + G_{19} + G_{23}) - (2G_8 + G_3 \\
 &\quad + G_7 + G_9)
 \end{aligned} \tag{11}$$

The gradient value of the final image is:

$$Gra = |Gra_x| + |Gra_y| \tag{12}$$

### 3.2 Small target signal enhancement algorithm based on morphology operation

The edge detection algorithm of Sobel operator can effectively enhance the small target signal of UAVs, and the background interference of large area and high brightness cloud can also be partially suppressed. In order to further reduce the interference of noise and gradient edge information, this paper introduces methods such as spatial domain filtering and morphological language to improve the signal strength of small targets.

First, convert the input RGB image into a grayscale image, and then use a bilateral filter to smooth the background<sup>[8]</sup>. Compared with the Gaussian filter, the kernel function of the bilateral filter not only considers the geometric distance between pixels, but also determines the weight value according to the gray difference of surrounding pixels. When the change of the image gray level is not obvious, the weight of the filter is mainly determined by the Euclidean distance between pixels, and the effect is similar to Gaussian blur. In the edge region where the gray value of the image changes greatly, the similarity of the gray level is small, and the pixel range within the range plays a leading role, which preserves the gradient information of the image. The output gray value in the bilateral filter is a weighted combination of surrounding gray values:

$$g(x, y) = \frac{\sum_{i,j} f(x, y) \omega(x, y, i, j)}{\sum_{i,j} \omega(x, y, i, j)} \tag{13}$$

$$\omega(x, y, i, j) = \exp\left(-\frac{(x-i)^2 + (y-j)^2}{2\sigma_d^2} - \frac{\|f(x, y) - f(i, j)\|}{2\sigma_r^2}\right) \quad (14)$$

Note:

$g(x, y)$ : the gray output value of center point coordinates;

$f(x, y)$ : the gray input value of the coordinate of the center point;

$\omega(x, y, i, j)$ : gray scale weight value of coordinate pixel points  $(i, j)$ ;

$\sigma_d$ : the standard deviation of the weight value in the spatial domain;

$\sigma_r$ : the standard deviation of the weighted value in the range.

After the bilateral filtering, part of the high-frequency noise is removed effectively, and the gradient characteristics of the image are retained. Then, the improved Sobel operator is used to extract the image gradient characteristics, and the contour range of the small UAV target is obtained. Then, a Gaussian filter is used to reduce the noise generated during the gradient detection.

At this time, the background interference of the image is partially suppressed and the dim target signal is effectively enhanced. However, there are still some narrow highlights at the edge of the cloud, and there are also some undetected parts of UAVs such as pores and gullies. This article introduces the morphological transformation operation, and first performs an etching operation on the image, and the narrow gullies and slender necks generated on the edges of large areas of clouds will be removed. Then the closing operation is carried out to eliminate small holes in the UAV target and to fill in the possible breaks between the rotor and the fuselage<sup>[8,9]</sup>. The basis of morphological operation is to define a structural unit  $B$  to operate on set  $A$ .

The corrosion of  $B$  to  $A$  is defined as:

$$A \ominus B = \{z | (B)_z \subseteq A\} \quad (15)$$

The expansion of  $B$  against  $A$  is defined as:

$$A \oplus B = \{z | (\hat{B})_z \cap A \neq \emptyset\} \quad (16)$$

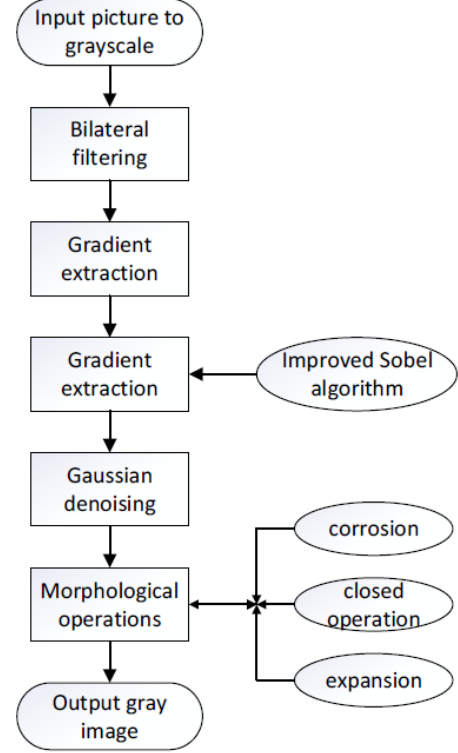


**Figure 6.** Spatial filtering and morphological image processing flow.

The closed operation of  $B$  on  $A$  is defined as:

$$A \bullet B = (A \oplus B) \ominus B \quad (17)$$

The structural unit  $B$  used for corrosion and expansion in this paper is a  $3 \times 3$  matrix, and the structural element used for closed operation is a  $25 \times 25$  elliptical kernel with an anchor point at the center. The above-mentioned spatial filtering, gradient extraction, and morphological transformation are sequentially performed on the input image to improve the signal-to-noise ratio of the image.

### 3.3 Target extraction method of adaptive threshold

Image segmentation is a process of dividing the image into several different regions according to different characteristics, so that the similarity within each region is maximized and the similarity between different regions is minimized. Threshold segmentation is the simplest method of gray image segmentation. When the average gray value of the background and the target is obviously different,

using threshold segmentation has a good effect.

$$f_{out}(x, y) = \begin{cases} g_1 & f_{in}(x, y) \geq thresh \\ g_0 & f_{in}(x, y) < thresh \end{cases} \quad (18)$$

The maximum inter-class variance method<sup>[10,11]</sup>, also known as the Otsu's method, is an unsupervised calculation method, which is often used to select the threshold value of a gray image. The principle is to traverse all gray values, and then calculate the variances between the classes, where the threshold  $t$  corresponding to the maximum  $s$  value is what is required:

$$s(t) = \lambda_0 \times \lambda_1 \times (u_0 - u_1)^2 \frac{1}{\sqrt{2\pi}\sigma} \exp\left(-\frac{(t - v_t)^2}{2\sigma^2}\right) \quad (19)$$

Note:

$\lambda_0$ : the proportion of the background region to the pixel points after segmentation by the threshold  $t$ ;

$\lambda_1$ : the proportion of the target region to the pixel points after segmentation;

$u_0$ : the average gray value of the background area after segmentation;

$u_1$ : the average gray value of the target area after segmentation.

If there is a significant target in the grayscale image obtained after the preliminary processing, the idea of the Otsu's method can be used for segmentation. In this paper, the image complexity parameter  $\theta$  is introduced as the evaluation standard, and it is considered that the pixel point of the grayscale value  $v > 5$  in the image is an effective pixel point  $n_0$ , which accounts for  $\theta$  of all pixel points in the total image. According to the size characteristics of the small UAV target in the image, when  $\theta > 0.3\%$ , it is considered that there may be a UAV target. Since the main purpose of segmentation is to separate the UAV target from some background interference, only the effective pixels will be calculated during the calculation of the threshold.

In the processed grayscale image, the UAV target area is more obvious due to its gradient char-

acteristics, and its grayscale value is larger in the image, and the value of the target area is not much different. Based on the characteristics of the gray value of the target area in each gray image, this paper considers that the most likely threshold is about the gray value  $v_t$  of the  $40 \times 40$  ( $1920 \times 1080$  resolution image). Gaussian distribution is introduced to adjust the calculation formula of the maximum variance between Otsu classes<sup>[12]</sup>:

$$s(t) = \lambda_0 \times \lambda_1 \times (u_0 - u_1)^2 \frac{1}{\sqrt{2\pi}\sigma} \exp\left(-\frac{(t - v_t)^2}{2\sigma^2}\right) \quad (20)$$

In Equation (20), Gaussian distribution is used to integrate the area size characteristics of UAVs in the image into the calculation of the maximum variance of interclass. After comparing and analyzing the images, the mean value  $v_t$  is determined by the small target size of the drone observed by the photoelectric equipment, and the variance  $\sigma$  is inversely proportional to the image complexity  $\theta$ . When the background in the image is cleaner, the complexity is smaller, indicating that the effect of early image processing is more obvious, the Otsu's method is less difficult to segment, and the variance value setting is relatively large. When there are many effective pixel points in the image and the background is complex, the variance value is relatively small. The small target size of the UAV plays a leading role in segmentation, so as to prevent the threshold setting from being too low and resulting in poor segmentation effect.

## 4. Discussion

The UAV detection method under the complex sky background requires real-time monitoring of small targets in the low altitude range. When an unknown moving object appears in the low altitude range, the system needs to obtain information of its distance, direction and height, and rotate the pearly head of the photoelectric equipment to obtain its appearance and morphological characteristics. In order to verify the effectiveness of the method presented in this paper, an experimental verification



platform is built to detect UAV targets in the sky background.

The experimental site was set up at a certain experimental base in Wuhan. The surrounding environment includes lakes, communities, and bridges, and the interference signal is relatively complicated. Drones were used and took off from different distances to make intrusion or escape movement. The radar captures the target's location, altitude, speed and other information, and the target radar map is obtained; and then the target and movement characteristics of the drone are used to screen out the possible drones. The target point, the UAV intrusion detection equipment building platform is shown in the **Figure 7**.



**Figure 7.** UAV intrusion detection equipment building platform.

After obtaining the video picture containing the suspicious target, in order to verify the detection and segmentation effect of the algorithm on small targets of UAVs, this paper conducted a lot of experiments in different environments. For the hardware configuration used, the CPU is Intel(R) Core i7-8750, running memory RAM is 16 G. The experiment is carried out with PYTHON and MATLAB under Windows10 (64-bit) system.

In this paper, several typical small target flying images of UAVs are selected in different environments and imaging modes, and the background suppression effect of the algorithm proposed in this paper and the traditional Sobel operator are compared. As shown in **Figure 8**, (a) is the visible light

camera image of the drone target flying in the long-distance range, (b) is the image captured by the infrared camera in the night environment, (c) is the picture obtained by the high-power laser supplement light equipment in the poor lighting environment. The four pictures in each group are the original picture, the three-dimensional effect grid of the original grayscale image, the grid calculated by the Sobel operator, and the grid processed by the overall algorithm of this article. The red box indicates the position of the small drone target in the image.

In order to further reflect the effect of the proposed algorithm on background suppression and significant small target enhancement, regional SNR and SNR gain are introduced for comparative verification. The higher the regional SNR is, the more significant the small target signal is. The larger the SNR gain is, the better the enhancement effect of the processing algorithm to the small target signal is. **Table 1** compares the effects of using the traditional Sobel operator with the algorithm of this paper.  $Std$  is the standard deviation of the gray value in the background area,  $(S/N)_{in}$  and  $(S/N)_{out}$  respectively represent the signal-to-noise ratio of the input and output images respectively, and  $(S/N)_{G1}$  represents the signal-to-noise ratio gain. From the data in the table, it can be seen that through the improvement of Sobel operator, spatial filtering and graphics transformation, the image signal-to-noise ratio has been significantly improved, and the performance of small targets is more significant, laying the foundation for target threshold segmentation.

The adaptive threshold segmentation method has a good adaptive effect to changing environmental conditions. Generally speaking, after the spatial filtering process of the RGB camera imaging, the complexity of the background is low, with less interference, and low calculated threshold; but when the threshold is used for the image after the infrared image and the high-power laser equipment fill light, the segmentation effect is often poor.

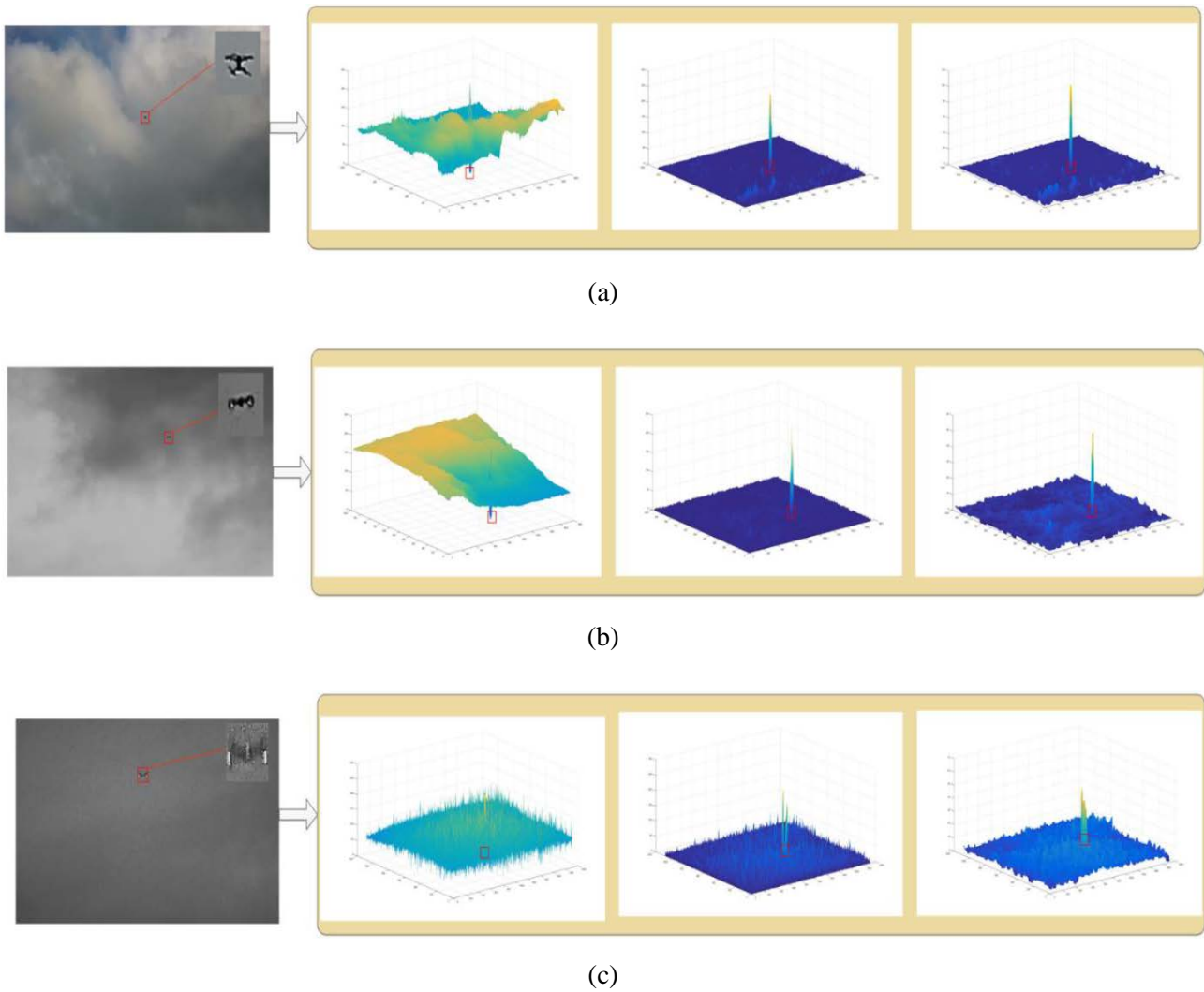


**Figure 8.** Comparison of effect between traditional gradient detection and the proposed algorithm.

**Table 1.** Comparison of signal-noise data between traditional gradient detection and the proposed algorithm

|         | The input image |              | Traditional Sobel operators |                |              | Algorithm of this paper |                |              |
|---------|-----------------|--------------|-----------------------------|----------------|--------------|-------------------------|----------------|--------------|
|         | $std_{in}$      | $(S/N)_{in}$ | $std_{out1}$                | $(S/N)_{out1}$ | $(S/N)_{G1}$ | $std_{out2}$            | $(S/R)_{out2}$ | $(S/N)_{G2}$ |
| Scene a | 26.73           | 1.08         | 5.49                        | 33.27          | 30.81        | 3.03                    | 58.08          | 53.78        |
| Scene b | 26.78           | 1.01         | 2.74                        | 40.14          | 39.74        | 1.51                    | 54.97          | 54.43        |
| Scene c | 10.30           | 0.18         | 5.58                        | 5.91           | 32.83        | 2.63                    | 10.41          | 57.83        |

As shown in **Figure 9**, under the conditions of infrared camera imaging, (a) is the original image, where the red box represents the location of the drone target; (b) is the filtered gray image, where the red box represents the target area to be segmented; (c) is the effect of segmentation by using the threshold value calculated from the grayscale image of the RGB camera. The threshold value is better in the segmentation effect of the RGB

camera. The red box is the target area, and the yellow box represents some mis-segmented areas. (d) is the threshold value calculated by the adaptive threshold segmentation algorithm for segmentation, and the red box is the target area. It can be seen that the adaptive threshold segmentation algorithm also has a better segmentation effect for changing environments.

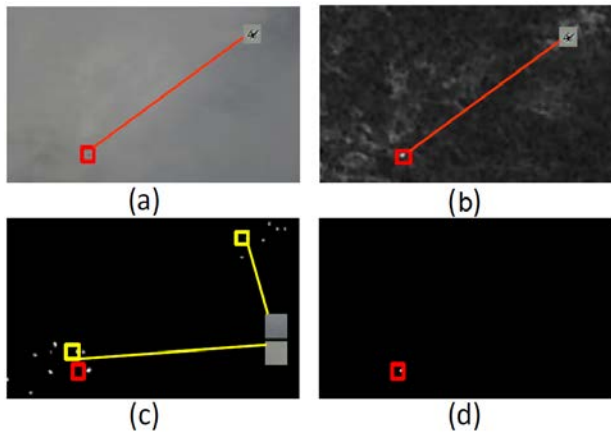


**Figure 9.** Comparison of the threshold segmentation effect.

## 5. Discussion

Aiming at the detection and segmentation of small UAV targets under complex sky background, this paper first proposes a multi-sensor information fusion model, which uses radar and photoelectric equipment to obtain the image and other characteristic information of the target in the sky; then it uses spatial filtering and gradient extraction and other operations to suppress the signal strength of the background noise and improve the signal-to-noise ratio of the target area. Finally, based on the Otsu's threshold segmentation algorithm, a segmentation method suitable for small UAV targets under the sky background is proposed. Experiments show that the spatial filtering-related operations can effectively enhance the small target signal, and the output gray image reflects the gray difference between the target and the background. In complex changing environments such as RGB camera imaging, infrared camera imaging, and high-power laser fill light, the threshold segmentation method also has good adaptability and has a good effect on the extraction of target regions in grayscale images. The research on the detection and segmentation technology of UAV small targets provides a detection basis for the prevention of UAV surveillance and low-altitude protection. It has important value in the military field and air defense in key areas.

## Conflict of interest

The authors declare that they have no conflict of interest.

## References

1. Zhang J, Zhang K, Wang J, *et al.* A survey on anti-UAV technology and its future trend. *Advances in Aeronautical Science and Engineering* 2018; 9(1): 1–8, 34. doi: 10.16615/j.cnki.1674-8190.2018.01.001.
2. Jiao S, Liu J, Wang B, Tian W. Fan wurenji fengqun zuozhan yunyong tanxi [Analysis on the application of anti-UAV swarm operations]. *Aerospace Technology* 2019; (2): 50–53, 64. doi: 10.16338/j.issn.1009-1319.20180198.
3. Chen C, Li C. On the problems in the small and light civil UAV security and the countermeasures. *Journal of Guangxi Police College* 2018; 31(4): 38–41.
4. He C, Ling J, Shi L. Current status and development of UAV detection and response technology. *Police Technology* 2019; (3): 4–7.
5. Yao B, Chen J. Research on anti-drone system based on multiple detection techniques. *China Association for Science and Technology, Ministry of Transport of the People's Republic of China, Chinese Academy of Engineering. Proceedings of the 2019 World Transport Conference*; 2019 Jun 13–16; Beijing. Beijing: China Highway Society; 2019. p. 1023–1025.
6. Shi X, Yang C, Xie W, *et al.* Anti-drone system with multiple surveillance technologies: Architecture, implementation, and challenges. *IEEE Communications Magazine* 2018; 56(4): 68–74.
7. Xia M, Zhao K, Ni W. Anti-UAV system and key technology for key point defense. *Command Control & Simulation* 2018; 40(2): 53–60, 71.
8. Sheu BH, Chiu CC, Lu WT, *et al.* Development of UAV tracing and coordinate detection method using a dual-axis rotary platform for an anti-UAV system. *Applied Sciences* 2019; 9(13): 2583. doi: 10.3390/app9132583.
9. Li P, Chen Q, Zheng H, He B. Anti-interference algorithm for clouds based on infrared small targets image. *Journal of Army Engineering University of PLA (Natural Science Edition)* 2011; 12(6): 588–

- 592.
10. Sheu BH, Chiu CC, Lu WT, *et al.* Dual-axis rotary platform with UAV image recognition and tracking. *Microelectronics Reliability* 2019; 95(Apr.): 8–17. doi: 10.1016/j.microrel.2019.02.005.
  11. Cao Y, Zhang Z, Zhong P, *et al.* Review on vision based intruder detection and recognition. *Computer Measurement & Control* 2019; 27(8): 7–11. doi: 10.16526/j.cnki.11-4762/tp.2019.08.002.
  12. Wang C, Wang T, Wang E, *et al.* Flying small target detection for anti-UAV based on a gaussian mixture model in a compressive sensing domain. *Sensors* 2019; 19(9): 2168. doi: 10.3390/s19092168.